Abstract We present an inverse power method for the computation of the first homogeneous eigenpair of the $p(x)$-Laplacian problem. The operators are discretized by the finite element method. The inner minimization problems are solved by a globally convergent inexact Newton method. Numerical comparisons are made, in one- and two-dimensional domains, with other results present in literature for the constant case $p(x) \equiv p$ and with other minimization techniques (namely, the nonlinear conjugate gradient) for the $p(x)$ variable case.

The inverse power method for the $p(x)$-Laplacian problem

M. Caliari · **S. Zuccher**

1 Introduction

In this paper we consider the generalization of the p-Laplacian eigenvalue problem with homogeneous Dirichlet boundary conditions

$$-\Delta_p u(x) = \eta_p \, |u(x)|^{p-2} \, u(x) \tag{1}$$

where $\Delta u(x) = \mathrm{div}(|\nabla u(x)|^{p-2} \nabla u(x))$, Ω is a bounded domain in $\mathbb{R}^d$, $u \in W_0^{1,p}(\Omega)$ and $p > 1$, to the case with variable exponent $p(x)$.

The p-Laplacian operator appears in several mathematical models that describe nonlinear problems in physics and mechanics [7, 9]. Examples include fluid dynamics [11], modeling of non-Newtonian fluids and glaciology [4, 10, 12, 20, 27, 28], turbulent flows [15], climatology [16], nonlinear diffusion (where the equation is called the N-diffusion equation, see Ref. [29] for the original article and Ref. [21] for some current developments), flows through porous media [30], power law materials [5] and torsional creep [24].

The p-Laplacian operator where p is replaced by $p(x)$, $1 < p^- \le p(x) \le p^+ < +\infty$, is deeply related to generalized Lebesgue and Sobolev spaces, which have been vigorously studied and whose theory has been ripe for applications to PDEs. The common assumption in literature is that the exponent $p(x)$ is a measurable function and $1/p(x)$ is globally log-Hölder continuous [17]. There have been many contributions to nonlinear elliptic problems associated with the $p(x)$-Laplacian from various view points (see Ref. [1, 2, 14] and Ref. [22] for a survey), whereas there are much less contributions to parabolic problems [3] and eigenvalue problems [18].

If p is constant, it is well known that the smallest eigenvalue satisfies

$$\underline{\eta_p} = \inf_{\substack{u \in W_0^{1,p}(\Omega) \\ u \ne 0}} \frac{\int_\Omega |\nabla u|^p \, \mathrm{d}x}{\int_\Omega |u|^p \, \mathrm{d}x}. \tag{2}$$

M. Caliari · S. Zuccher
Department of Computer Science, University of Verona, Strada Le Grazie 15, 37134, Verona, Italy

M. Caliari
E-mail: marco.caliari@univr.it

S. Zuccher
E-mail: simone.zuccher@univr.it

The trivial generalization of quotient (2) to the case $p = p(x)$ yields a problem in which the homogeneity is lost, that is if u is a minimizer then ωu, $\omega \neq 0$, is not. In Ref. [19], the homogeneity is restored considering

$$\underline{\lambda} = \inf_{\substack{u \in W_0^{1,p(x)}(\Omega) \\ u \neq 0}} \frac{\|\nabla u\|_{p(x)}}{\|u\|_{p(x)}},$$

where the norm $\|\cdot\|_{p(x)}$ is the so called *Luxemburg norm*

$$\|u\|_{p(x)} = \inf_{\gamma > 0} \left\{ \gamma : \int_\Omega \left| \frac{u(x)}{\gamma} \right|^{p(x)} \frac{\mathrm{d}x}{p(x)} \leq 1 \right\}. \tag{3}$$

The use of $p(x)^{-1}\mathrm{d}x$ (rather than the classical $\mathrm{d}x$) just simplifies the equations a little (see Ref. [19]). The corresponding Euler–Lagrange equation is

$$-\operatorname{div}\left(\left| \frac{\nabla u(x)}{\|\nabla u\|_{p(x)}} \right|^{p(x)-2} \frac{\nabla u(x)}{\|\nabla u\|_{p(x)}} \right) = \lambda T \left| \frac{u(x)}{\|u\|_{p(x)}} \right|^{p(x)-2} \frac{u(x)}{\|u\|_{p(x)}}, \tag{4}$$

where

$$T = \frac{\int_\Omega \left| \frac{\nabla u(x)}{\|\nabla u\|_{p(x)}} \right| \mathrm{d}x}{\int_\Omega \left| \frac{u(x)}{\|u\|_{p(x)}} \right| \mathrm{d}x}.$$

We notice that in the constant case $p(x) \equiv p$, since $p\|u\|_p^p = \|u\|_{L^p}^p$,

$$(\lambda, u) \text{ eigenpair for (4)} \Leftrightarrow (\lambda^p, u/\sqrt[p]{p}) \text{ eigenpair for (1)} \tag{5}$$

with $\|u\|_p = \left\|u/\sqrt[p]{p}\right\|_{L^p} = 1$.

Although some different numerical methods for the eigenvalue problem with constant p are available, see Ref. [7, 9, 13], to the knowledge of the authors the first numerical method, based on the nonlinear conjugate gradient method, for computing

$$\underline{\lambda}^2 = \Lambda = \inf_{\substack{u \in W_0^{1,p(x)}(\Omega) \\ u \neq 0}} \frac{\|\nabla u\|_{p(x)}^2}{\|u\|_{p(x)}^2} \tag{6}$$

and the corresponding minimizer was proposed by the first author in Ref. [6], where only the case $p(x) \geq 2$ was considered. Here we use a preconditioned quadratic model for the minimization problem, either with the exact Hessian, if $p(x) \geq 2$, or with a modified Hessian, otherwise. The new method turns out to be more general, more robust and faster (see the numerical experiments in Table 3, Section 3) than the previous one.

2 The inverse power method for a nonlinear eigenproblem

Given $R\colon \mathbb{R}^n \to \mathbb{R}_+$ and $S\colon \mathbb{R}^n \to \mathbb{R}_+$ convex, differentiable, even and positively 2-homogeneous functionals, with the further assumption that $S(u) = 0$ only if $u = 0$, then the critical points u^* of $F(u) = R(u)/S(u)$ satisfy

$$\nabla_u F(u^*) = \nabla_u R(u^*) - \frac{R(u^*)}{S(u^*)} \nabla_u S(u^*) = 0.$$

If we define $r(u) = \nabla_u R(u)$, $s(u) = \nabla_u S(u)$ and $\Lambda^* = \frac{R(u^*)}{S(u^*)}$, then the critical point u^* satisfies the *nonlinear eigenproblem*

$$r(u^*) - \Lambda^* s(u^*) = 0. \tag{7}$$

If $R(u) = \langle u, Au \rangle$, where $A\colon \mathbb{R}^n \to \mathbb{R}^n$ is linear and $S(u) = \langle u, u \rangle$, $\langle \cdot, \cdot \rangle$ being the scalar product in $\mathbb{R}^n \times \mathbb{R}^n$, the standard linear eigenproblem is retrieved. The generalization of the inverse power method for the computation of the smallest eigenvalues is the following algorithm:

1. take $\tilde{u}^0$ random and compute $u^0 = \dfrac{\tilde{u}^0}{S(\tilde{u}^0)^{1/2}}$ and $\Lambda^0 = F(u^0) = R(u^0)$

2. repeat
   - $\tilde{u}^k = \arg\min\limits_u \{R(u) - \langle u, s(u^{k-1}) \rangle\}$
   - $u^k = \dfrac{\tilde{u}^k}{S(\tilde{u}^k)^{1/2}}$
   - $\Lambda^k = F(u^k) = R(u^k)$
   until convergence

It is proven [23] that the sequence $\{(u^k, \Lambda^k)\}_k$ produced by the algorithm satisfies $F(u^k) < F(u^{k-1})$ and converges to an eigenpair (u^*, Λ^*) for problem (7), with u^* a critical point of F.

Let now $u(x)$ be a linear combination of basis functions

$$u(x) = \sum_{j=1}^n u_j \phi_j(x),$$

with $u = (u_1, \ldots, u_n)^{\mathrm{T}}$ the vector of coefficients, and let us apply the algorithm described above to the case

$$R(u) = \left\| \sum_{j=1}^n u_j \nabla \phi_j(\cdot) \right\|_{p(x)}^2, \quad S(u) = \left\| \sum_{j=1}^n u_j \phi_j(\cdot) \right\|_{p(x)}^2$$

In our numerical experiments, the set of functions $\{\phi_j(x)\}_{j=1}^n$ will be a proper set of finite element basis functions. With abuse of notation, we will write for short $R(u) = \|\nabla u\|_{p(x)}^2$ and $S(u) = \|u\|_{p(x)}^2$.

We remind that the algorithm does not guarantee the convergence to the smallest eigenvalue. On the other hand, it is possible to apply it to different initial guesses and then take the smallest eigenvalue.

2.1 Initial values and exit criteria

Although $\tilde{u}^0$ can be chosen randomly, it is clear that the more it is close to u^*, the faster the algorithm converges. In order to speed up the convergence, we use a continuation technique over $p(x)$, starting from $p(x) \equiv 2$ for which the solution is known at least for common domains Ω. By employing a convex combination

$$p^m(x) = 2 \cdot (1 - \theta_m) + p(x) \cdot \theta_m, \quad \theta_m = \sqrt{\frac{m}{M}}, \quad m = 0, 1, \ldots, M, \tag{8}$$

m-th problem is solved by providing as initial condition the solution of $(m-1)$-th problem.

For the minimization problem (called *inner problem*)

$$\tilde{u}^k = \arg\min_u \{R(u) - \langle u, s(u^{k-1})\rangle\}, \quad \text{given } u^{k-1}$$

we use an iterative method as well. Since the inverse power method, at convergence, ensures

$$r(u^{k-1}) - \Lambda^{k-1} s(u^{k-1}) \approx 0 \Rightarrow r\left(\frac{u^{k-1}}{\Lambda^{k-1}}\right) - s(u^{k-1}) \approx 0,$$

and (at each iteration)

$$r(\tilde{u}^k) - s(u^{k-1}) = 0,$$

a good choice for the initial value of $\tilde{u}^k$ is u^{k-1}/Λ^{k-1}. By the proof of Lemma 3.1 in Ref. [23], we know that the descent in F is guaranteed not only for the exact solution of the inner problem but also for any vector $\bar{u}^k$ which satisfies the condition

$$R(\bar{u}^k) - \langle \bar{u}^k, s(u^{k-1})\rangle < R\left(\frac{u^{k-1}}{F(u^{k-1})}\right) - \left\langle \frac{u^{k-1}}{F(u^{k-1})}, s(u^{k-1})\right\rangle.$$

Since $F(u^{k-1}) = \Lambda^{k-1}$, $u^{k-1}/F(u^{k-1})$ is precisely the above suggested choice for the initial value of $\tilde{u}^k$. Therefore, in principle, starting from this value, the use of a descent method for the inner problem would require a single step in order to guarantee the descent in F. More realistically, this means that far from convergence (for instance during the continuation technique) it makes no sense to solve the inner problem too accurately. For this reason, an exit criterion could encompass both a relatively large tolerance and a relatively small maximum number of iterations.

A classical exit criterion for the inverse power method is

$$\left|\Lambda^k - \Lambda^{k-1}\right| \leq \text{tol} \cdot \left|\Lambda^k\right| \tag{9}$$

for a given tolerance tol. As soon as it is satisfied, we assume that $\Lambda^k \approx \Lambda^*$ and thus

$$r(u^k) - \Lambda^k s(u^k) \approx 0. \tag{10}$$

We call the left hand side *residual*; clearly, its infinity norm could be used as a different exit criterion.

2.2 Approximation of the Luxemburg norm

If $u(x)$ is not zero almost everywhere, then its Luxemburg norm γ is implicitly defined by

$$F(u,\gamma) = \int_\Omega \left| \frac{u(x)}{\gamma} \right|^{p(x)} \frac{\mathrm{d}x}{p(x)} - 1 = 0. \tag{11}$$

Hereafter we remove the integration domain Ω from the notation. The derivative with respect to γ of $F(u,\gamma)$ is

$$\partial_\gamma F(u,\gamma) = -\frac{1}{\gamma} \int \left| \frac{u(x)}{\gamma} \right|^{p(x)} \mathrm{d}x \tag{12}$$

and thus Newton's method can be easily applied. For a given $u(x)$, $F(u,\gamma)$ is a monotonically decreasing convex $\mathscr{C}^2$ function in γ. This guarantees the convergence of Newton's method whenever the initial guess $\gamma_0 > 0$ is chosen such that $F(u,\gamma_0) \geq 0$. For the initial guess γ_0, we use the following estimates

$$\gamma_0 = \begin{cases} \left(\int_\Omega \frac{|u(x)|^{p(x)}}{p(x)} \mathrm{d}x \right)^{\frac{1}{p_{\max}}} & \text{if } \int_\Omega \frac{|u(x)|^{p(x)}}{p(x)} \mathrm{d}x \geq 1 \\[3ex] \left(\int_\Omega \frac{|u(x)|^{p(x)}}{p(x)} \mathrm{d}x \right)^{\frac{1}{p_{\min}}} & \text{if } \int_\Omega \frac{|u(x)|^{p(x)}}{p(x)} \mathrm{d}x < 1 \end{cases}$$

where $p_{\max} = \max p(x)$ and $p_{\min} = \min p(x)$. In fact, if we consider the first case,

$$F(u,\gamma_0) = \int_\Omega \left| \frac{u(x)}{\gamma_0} \right|^{p(x)} \frac{\mathrm{d}x}{p(x)} - 1 \geq \int_\Omega \frac{|u(x)|^{p(x)}}{\gamma_0^{p_{\max}}} \frac{\mathrm{d}x}{p(x)} - 1 =$$

$$= \frac{1}{\int_\Omega \frac{|u(x)|^{p(x)}}{p(x)} \mathrm{d}x} \int_\Omega |u(x)|^{p(x)} \frac{\mathrm{d}x}{p(x)} - 1 = 0.$$

2.3 The inner problem

In the inverse power method, we need to solve the inner problem

$$\tilde{u}^k = \arg\min_u f(u) = \arg\min_u \{ R(u) - \langle u, s(u^{k-1}) \rangle \}, \quad \text{given } u^{k-1}.$$

We first compute $\langle v, s(u) \rangle = \langle v, \nabla_u S(u) \rangle$ for given vectors u and v. Since $\gamma(u) = \|u\|_{p(x)}$ is implicitly defined by $F(u,\gamma(u)) = 0$, the differentiation of implicit functions leads to

$$\langle v, \nabla_u F(u,\gamma(u)) \rangle = \langle v, \partial_u F(u,\gamma(u)) \rangle + \langle v, \partial_\gamma F(u,\gamma(u)) \nabla_u \gamma(u) \rangle = 0,$$

from which

$$\langle v, \nabla_u \|u\|_{p(x)} \rangle = \langle v, \nabla_u \gamma(u) \rangle = -\frac{\langle v, \partial_u F(u,\gamma(u)) \rangle}{\partial_\gamma F(u,\gamma(u))}.$$

By recalling that, in general,

$$\partial_{u_i} \left(\int g(u(x)) \mathrm{d}x \right) = \int g'(u(x)) \phi_i(x) \mathrm{d}x,$$

for $v(x) = \sum_{j=1}^{n} v_j \phi_j(x)$ we have

$$\langle v, \partial_{u_i} \left(\int g(u(x)) \mathrm{d}x \right) \rangle = \int g'(u(x)) v(x) \mathrm{d}x$$

and thus

$$\langle v, \partial_u F(u, \gamma) \rangle = \int \left| \frac{u(x)}{\gamma} \right|^{p(x)-2} \frac{u(x)}{\gamma} \frac{v(x)}{\gamma} \mathrm{d}x.$$

By employing (12) we get

$$\langle v, \nabla_u \|u\|_{p(x)} \rangle = \frac{\int \left| \frac{u(x)}{\|u\|_{p(x)}} \right|^{p(x)-2} \frac{u(x)}{\|u\|_{p(x)}} v(x) \mathrm{d}x}{\int \left| \frac{u(x)}{\|u\|_{p(x)}} \right|^{p(x)} \mathrm{d}x},$$

from which

$$\langle v, s(u) \rangle = \langle v, 2 \|u\|_{p(x)} \nabla_u \|u\|_{p(x)} \rangle = 2 \frac{\int \left| \frac{u(x)}{\|u\|_{p(x)}} \right|^{p(x)-2} u(x) v(x) \mathrm{d}x}{\int \left| \frac{u(x)}{\|u\|_{p(x)}} \right|^{p(x)} \mathrm{d}x}. \tag{13}$$

Given u^{k-1} of unitary Luxemburg norm, the problem reduces to find the minimizer of

$$f(u) = R(u) - \langle u, s(u^{k-1}) \rangle =$$

$$= \|\nabla u\|_{p(x)}^2 - 2 \frac{\int |u^{k-1}(x)|^{p(x)-2} u^{k-1}(x) u(x) \mathrm{d}x}{\int |u^{k-1}(x)|^{p(x)} \mathrm{d}x} \tag{14}$$

We use a line search method based on the *sufficient decrease* condition. If u_c is the solution at the current iteration, its update is

$$u_+ = u_c + \delta d, \tag{15}$$

where d is a descent direction, i.e. $\langle \nabla_u f(u_c), d \rangle < 0$, and δ is such that

$$f(u_c + \delta d) < f(u_c) + \alpha \delta \langle \nabla_u f(u_c), d \rangle \tag{16}$$

with $\alpha = 10^{-4}$. Condition (16) is usually called Armijo's rule.

2.3.1 The quadratic model for the inner problem, $p(x) \geq 2$

We first consider the case $p(x) \geq 2$ and approximate $f(u)$ in (14) with a quadratic model

$$f(u) \approx f(u_c) + \langle \nabla_u f(u_c), u - u_c \rangle + \frac{1}{2} \langle u - u_c, H(u_c)(u - u_c) \rangle$$

where $H(u_c)$ is the exact Hessian of f at the current iteration u_c. For $p(x) \geq 2$, $R(u)$ is twice continuously differentiable and convex, i.e. the Hessian of f is symmetric positive definite. Therefore

$$\nabla_u f(u_+) \approx \nabla_u f(u_c) + H(u_c)(u_+ - u_c) = 0 \Leftrightarrow u_+ - u_c = -H(u_c)^{-1} \nabla_u f(u_c)$$

and hence the descent direction is $d = -H(u_c)^{-1}\nabla_u f(u_c)$. If condition (16) is not satisfied for a given δ, then it is repeatedly reduced *(backtracking)* until the condition is satisfied, using a quite standard cubic polynomial model for $p(\delta) = f(u_c + \delta d)$ (see Ref. [26]).

Let us compute $\nabla_u f(u)$ and $H(u)v$, for a given $v \in \mathbb{R}^n$. With the arguments used to obtain (13), we immediately have

$$r_i(u) = \partial_{u_i} R(u) = 2 \frac{\|\nabla u\|_{p(x)} \int \left| \frac{\nabla u(x)}{\|\nabla u\|_{p(x)}} \right|^{p(x)-2} \frac{\nabla u(x)}{\|\nabla u\|_{p(x)}} \cdot \nabla \phi_i(x) \mathrm{d}x}{\int \left| \frac{\nabla u(x)}{\|\nabla u\|_{p(x)}} \right|^{p(x)} \mathrm{d}x} \tag{17}$$

where here $\cdot$ denotes the scalar product in $\mathbb{R}^d \times \mathbb{R}^d$. Since u^{k-1} has unitary Luxemburg norm,

$$\partial_{u_i} f(u) = 2 \frac{K \int \left| \frac{\nabla u}{K} \right|^{p-2} \frac{\nabla u}{K} \cdot \nabla \phi_i}{\int \left| \frac{\nabla u}{K} \right|^{p}} - 2 \frac{\int |u^{k-1}|^{p-2} u^{k-1} \phi_i}{\int |u^{k-1}|^{p}} \tag{18}$$

where we set $K = \|\nabla u\|_{p(x)}$ and omitted the dependency on x in the integrals in order to reduce the notation. By introducing

$$N_i(u) = \int \left| \frac{\nabla u}{K} \right|^{p-2} \nabla u \cdot \nabla \phi_i, \quad D(u) = \int \left| \frac{\nabla u}{K} \right|^{p}$$

the i-th row of $H(u)v$ is

$$(H(u)v)_i = 2 \frac{D(u)\langle v, \nabla_u N_i(u)\rangle - N_i(u)\langle v, \nabla_u D(u)\rangle}{D(u)^2} =$$

$$= 2 \frac{\int (p-2)\left| \frac{\nabla u}{K} \right|^{p-4} \frac{\nabla u}{K} \cdot \frac{\nabla v K - \nabla u \langle v, \nabla_u K\rangle}{K^2} \nabla u \cdot \nabla \phi_i + \left| \frac{\nabla u}{K} \right|^{p-2} \nabla v \cdot \nabla \phi_i}{D(u)} +$$

$$- 2 \frac{N_i(u) \int p \left| \frac{\nabla u}{K} \right|^{p-2} \frac{\nabla u}{K} \cdot \frac{\nabla v K - \nabla u \langle v, \nabla_u K\rangle}{K^2}}{D(u)^2} =$$

$$= 2 \frac{\int (p-2)\left| \frac{\nabla u}{K} \right|^{p-4} \frac{\nabla u}{K} \cdot \nabla v \frac{\nabla u}{K} \cdot \nabla \phi_i}{D(u)} +$$

$$- 2 \frac{\langle v, \nabla_u K\rangle \int (p-2)\left| \frac{\nabla u}{K} \right|^{p-2} \frac{\nabla u}{K} \cdot \nabla \phi_i}{D(u)} + 2 \frac{\int \left| \frac{\nabla u}{K} \right|^{p-2} \nabla v \cdot \nabla \phi_i}{D(u)} +$$

$$- 2 \frac{\frac{N_i(u)}{K} \int p \left| \frac{\nabla u}{K} \right|^{p-2} \frac{\nabla u}{K} \cdot \nabla v}{D(u)^2} + 2 \frac{\frac{N_i(u)}{K} \langle v, \nabla_u K\rangle \int p \left| \frac{\nabla u}{K} \right|^{p}}{D(u)^2}.$$

By using again (13), the inner product $\langle v, \nabla_u K\rangle$ can be recast as

$$\langle v, \nabla_u K\rangle = \frac{\int \left| \frac{\nabla u}{K} \right|^{p-2} \frac{\nabla u}{K} \cdot \nabla v}{D(u)}$$

and the i-th row of $H(u)v$ becomes

$$
(H(u)v)_i = 2 \frac{\int (p-2) \left| \frac{\nabla u}{K} \right|^{p-4} \frac{\nabla u}{K} \cdot \nabla v \frac{\nabla u}{K} \cdot \nabla \phi_i}{D(u)} +
$$
$$
- 2 \frac{\int \left| \frac{\nabla u}{K} \right|^{p-2} \frac{\nabla u}{K} \cdot \nabla v \int (p-2) \left| \frac{\nabla u}{K} \right|^{p-2} \frac{\nabla u}{K} \cdot \nabla \phi_i}{D(u)^2} +
$$
$$
+ 2 \frac{\int \left| \frac{\nabla u}{K} \right|^{p-2} \nabla v \cdot \nabla \phi_i}{D(u)} +
$$
$$
- 2 \frac{\int \left| \frac{\nabla u}{K} \right|^{p-2} \frac{\nabla u}{K} \cdot \nabla \phi_i \int p \left| \frac{\nabla u}{K} \right|^{p-2} \frac{\nabla u}{K} \cdot \nabla v}{D(u)^2} +
$$
$$
+ 2 \frac{\int \left| \frac{\nabla u}{K} \right|^{p-2} \frac{\nabla u}{K} \cdot \nabla \phi_i \int \left| \frac{\nabla u}{K} \right|^{p-2} \frac{\nabla u}{K} \cdot \nabla v \int p \left| \frac{\nabla u}{K} \right|^p}{D(u)^3}. \quad (19)
$$

The reason for computing the action of $H(u)$ to a vector is that $H(u)$ is not a sparse matrix, even if finite elements are used. Therefore, the descent direction $-H(u_c)^{-1}\nabla_u f(u_c)$ is computed through an iterative method such as the preconditioned conjugate gradient method, which only requires the action of $H(u_c)$ to a vector v. A good choice for the preconditioner in computing $\tilde{u}^k$ can be suggested by the modified gradient

$$
\partial_{u_i} f_c(u) = 2 \frac{\int \left| \frac{\nabla u_c}{K_c} \right|^{p-2} \nabla u \cdot \nabla \phi_i}{\int \left| \frac{\nabla u_c}{K_c} \right|^p} - 2 \frac{\int \left| u^{k-1} \right|^{p-2} u^{k-1} \phi_i}{\int \left| u^{k-1} \right|^p}
$$

and the corresponding modified Hessian H_c, whose entries are

$$
2 \frac{\int \left| \frac{\nabla u_c}{K_c} \right|^{p-2} \nabla \phi_j \cdot \nabla \phi_i}{\int \left| \frac{\nabla u_c}{K_c} \right|^p}. \quad (20)
$$

In fact, this preconditioner turns out to be sparse in case the basis functions $\{\phi_j(x)\}$ correspond to a finite element method. It is possible to use a fixed preconditioner for each iteration of the inverse power method (and not a preconditioner for each iteration of the inner problem), starting from the modified gradient

$$
\partial_{u_i} f^{k-1}(u) = 2 \frac{\int \left| \frac{\nabla u^{k-1}}{K^{k-1}} \right|^{p-2} \nabla u \cdot \nabla \phi_i}{\int \left| \frac{\nabla u^{k-1}}{K^{k-1}} \right|^p} - 2 \frac{\int \left| u^{k-1} \right|^{p-2} u^{k-1} \phi_i}{\int \left| u^{k-1} \right|^p}
$$

and the corresponding modified Hessian H_{k-1}, whose entries are

$$
2 \frac{\int \left| \frac{\nabla u^{k-1}}{K^{k-1}} \right|^{p-2} \nabla \phi_j \cdot \nabla \phi_i}{\int \left| \frac{\nabla u^{k-1}}{K^{k-1}} \right|^p}. \quad (21)
$$

Once the modified Hessian is computed, it is factorized by Choleski's method and the triangular factors are inverted in order to get the preconditioned conjugate gradient iterations.

2.3.2 The quadratic model for the inner problem, $p(x) \geq p^- > 1$

If, for some values of x, $p(x)$ is less than two and $\nabla u(x)$ is zero, than the first and the third term in the Hessian (19) are not defined, while the gradient (18) is still well defined, in the sense that

$$|\nabla u(x)|^{p(x)-2} \nabla u(x) \cdot \nabla \phi_i(x) = 0 \quad \text{if} \quad \nabla u(x) = 0.$$

We can consider (see Ref. [9]) the modified Hessian arising from

$$N_i^{\varepsilon_n}(u) = \int \left(\varepsilon_n^2 + \left| \frac{\nabla u}{K} \right|^2 \right)^{\frac{p-2}{2}} \nabla u \cdot \nabla \phi_i, \quad D(u) = \int \left| \frac{\nabla u}{K} \right|^p$$

where ε_n is a small quantity, possibly depending on the number n of basis functions $\phi_j(x)$

$$2 \frac{\int (p-2) \left(\varepsilon_n^2 + \left| \frac{\nabla u}{K} \right|^2 \right)^{\frac{p-4}{2}} \frac{\nabla u}{K} \cdot \nabla v \frac{\nabla u}{K} \cdot \nabla \phi_i}{D(u)} +$$

$$-2 \frac{\int \left| \frac{\nabla u}{K} \right|^{p-2} \frac{\nabla u}{K} \cdot \nabla v \int (p-2) \left(\varepsilon_n^2 + \left| \frac{\nabla u}{K} \right|^2 \right)^{\frac{p-2}{2}} \frac{\nabla u}{K} \cdot \nabla \phi_i}{D(u)^2} +$$

$$+2 \frac{\int \left(\varepsilon_n^2 + \left| \frac{\nabla u}{K} \right|^2 \right)^{\frac{p-2}{2}} \nabla v \cdot \nabla \phi_i}{D(u)} +$$

$$-2 \frac{\int \left(\varepsilon_n^2 + \left| \frac{\nabla u}{K} \right|^2 \right)^{\frac{p-2}{2}} \frac{\nabla u}{K} \cdot \nabla \phi_i \int p \left| \frac{\nabla u}{K} \right|^{p-2} \frac{\nabla u}{K} \cdot \nabla v}{D(u)^2} +$$

$$+2 \frac{\int \left(\varepsilon_n^2 + \left| \frac{\nabla u}{K} \right|^2 \right)^{\frac{p-2}{2}} \frac{\nabla u}{K} \cdot \nabla \phi_i \int \left| \frac{\nabla u}{K} \right|^{p-2} \frac{\nabla u}{K} \cdot \nabla v \int p \left| \frac{\nabla u}{K} \right|^p}{D(u)^3}$$

We notice that, in this way, the integrand function of the first term above side is equal to zero where $\nabla u(x) = 0$, and well defined otherwise, even without ε_n^2. Therefore we replace

$$\varepsilon_n^2 + \left| \frac{\nabla u}{K} \right|^2$$

with

$$(1 - \text{sign} |\nabla u|^2) + \left| \frac{\nabla u}{K} \right|^2$$

in that term. Indeed, such a modification is useful in the numerical implementation of f, its gradient and its exact Hessian, even in the case $p(x) \geq 2$, for the evaluation of terms (see, for instance, the second, the fourth and the fifth above) like

$$|z|^{p-2} z,$$

which can be numerically computed as

$$((1-\operatorname{sign}|z|^2)+|z|^2)^{\frac{p-2}{2}}z.$$

On the other hand, if $\nabla u(x)=0$, the third term in the Hessian above is not defined without ε_n^2, but it is well defined if $\nabla u(x)\neq 0$. Therefore, we replace

$$\varepsilon_n^2+\left|\frac{\nabla u}{K}\right|^2$$

in the third term of the Hessian above and in the corresponding modified Hessian (see (20)) with

$$\varepsilon_n^2\cdot(1-\operatorname{sign}|\nabla u|^2)+\left|\frac{\nabla u}{K}\right|^2.$$

When $p(x)\to 1^+$ for some values of x, the eigenvalue problem is numerically quite difficult. This is due not only to the fact that the exact Hessian does not exist, but also to the high derivatives of the solution at the boundaries. In fact, as reported in Figure 1 for the case of p constant, when $p\to 1^+$ the first eigenfunction on the ball converges to its characteristic function (see Ref. [25]).

3 Numerical results

3.1 Details of the algorithm

For the computation of the Luxemburg norm, Newton's method is stopped when the relative difference of two successive solutions is smaller then $10\cdot\varepsilon$, where ε is the machine precision.

From our numerical experience, we found that a number of continuation steps in (8) chosen as

$$M=\begin{cases}\left\lceil\dfrac{\max p(x)}{2}\right\rceil & \text{if }\min p(x)\geq 2\\[2ex]\lceil-3\log(\min p(x)-1)\rceil & \text{if }\min p(x)<2\end{cases}$$

provides a satisfactory behavior. Moreover, the m-th problem in (8) is solved with tolerance

$$\text{tol}_m=\text{tol}_0\cdot(1-\theta_m)+\text{tol}\cdot\theta_m$$

where $\text{tol}_0=100\cdot\text{tol}$ and tol is the tolerance in the exit criterion (9) for the inverse power method. It is chosen proportional to h^{r+1}, where r is the degree of the finite element piecewise polynomial basis. The same tolerance is used for inner problem (14). Four exit criteria are used. Since we use (modified) Newton's method, if the infinity norm of the descent direction δd in (15) is smaller than $\text{tol}\cdot\|u_c\|_\infty$ already with $\delta=1$, we stop the iterations. Then we consider the ratio between the relative change in $f(u_+)$ and the relative change in u_+. If

$$\left\|\frac{\nabla_u f(u_+)\circ u_+}{f(u_+)}\right\|_\infty\leq\text{tol},$$

where $\circ$ denotes Hadamard's product, we stop the iterations. We stop the iterations if the method stagnates, that is if $\|\delta d\|_\infty\leq 0.1\cdot\text{tol}\|u_c\|_\infty$, too. Finally, we fix the maximum number of iterations to 10. The value of ε_n for the modified Hessian is 10^{-5}.

3.2 One-dimensional case

We implemented and run the one-dimensional case in GNU Octave 3.8, using piecewise linear basis functions $\phi_j(x)$ and approximating the arising integrals by midpoint quadrature formulas.

The initial solution $u^0(x)$ corresponding to $p(x) \equiv p = 2$ is the (piecewise linear interpolation of the) first eigenfunction of

$$-u''(x) = \eta_2 u(x), \quad x_0 < x < x_1$$

normalized in order to have $\|u^0\|_2 = 1$, that is

$$u^0(x) = \frac{2}{\sqrt{x_1 - x_0}} \sin\left(\frac{x - x_0}{x_1 - x_0}\pi\right), \quad \eta_2 = \underline{\eta_2} = \left(\frac{\pi}{x_1 - x_0}\right)^2.$$

p	$\underline{\lambda}^p$	$\left|\underline{\eta}_p - \underline{\lambda}^p\right| / \underline{\eta}_p$
1.1	1.28	8.6e-05
1.2	1.46	1.9e-05
1.3	1.61	4.8e-05
1.4	1.75	5.9e-05
1.5	1.88	6.5e-05
1.6	2.00	6.8e-05
1.7	2.12	7.1e-05
1.8	2.24	7.5e-05
1.9	2.35	7.8e-05
2.0	2.47	8.2e-05
3.0	3.54	1.6e-04
4.0	4.56	3.0e-04
5.0	5.58	5.1e-04
6.0	6.59	8.0e-04
7.0	7.59	1.2e-03
8.0	8.59	1.6e-03
9.0	9.59	2.1e-03
10.0	10.59	2.6e-03

Table 1 Values of $\underline{\lambda}^p$ and relative error with respect to $\underline{\eta}_p$ for some values of constant $p(x) \equiv p$, in the interval $(-1, 1)$.

The first test aims at comparing our results with the analytical solution, which is known for constant values of $p(x) \equiv p$ in the interval $(-1, 1)$ (see, for instance, Ref. [8])

$$\underline{\eta}_p = \left(\frac{2\sqrt[p]{p-1}(\pi/p)}{2\sin(\pi/p)}\right)^p.$$

Table 1 reports the eigenvalue $\underline{\lambda}^p$, computed with 101 basis functions, and the relative difference with the corresponding analytical value $\underline{\eta}_p$ (see (5)). Figure 1 shows the eigenfunction $u(x)$ for different values of constant p. In the limit $p \to 1^+$ it tends to an almost constant function with steep gradients at the boundaries due to the homogeneous boundary conditions, whereas in the limit $p \to +\infty$ the eigenfunction resembles the absolute value of a linear function (non differentiable at the origin).
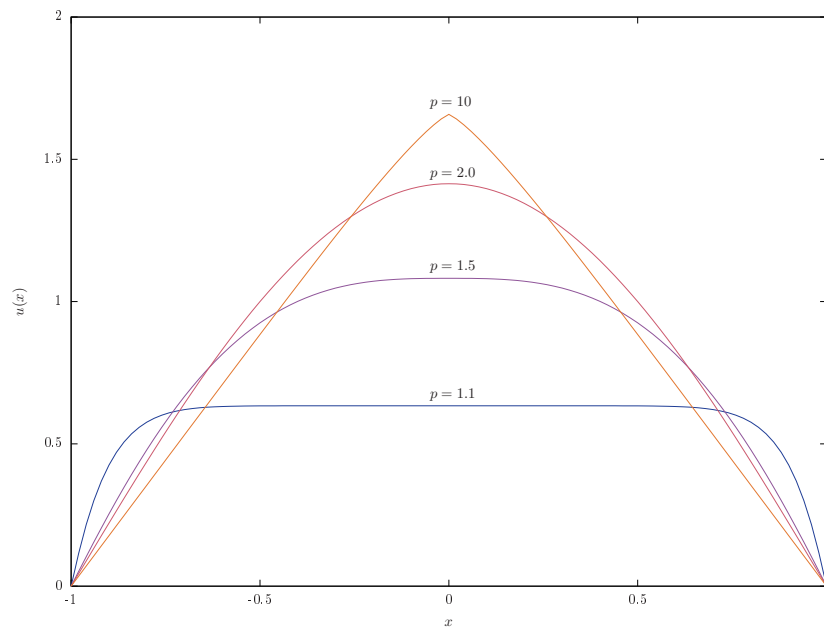
Fig. 1 First eigenfunctions for some values of constant $p(x) \equiv p$.
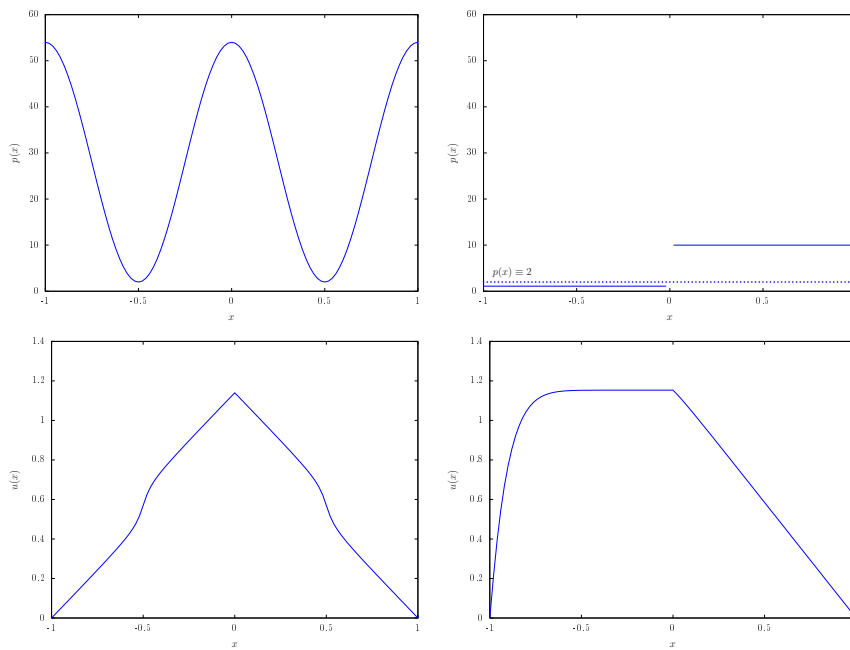
Fig. 2 $p(x) = 28 + 26\cos(2\pi x)$ (left) and $p(x) = 1.1$ if $x < 0$ and $p(x) = 10$ if $x \geq 0$ (right) and the corresponding eigenfunctions (bottom).

Figure 2 reports the first eigenfunction for two cases. In the first one (left), $p(x) = 28 + 26\cos(2\pi x)$, in the second one (right) $p(x)$ is discontinuous, $p(x) = 1.1$ if $x < 0$ and $p(x) = 10$ otherwise. The second case, although does not satisfy the log-Hölder continuity usually required to the exponent, was chosen as a limit case to check the robustness of the method. The values of $\underline{\lambda}$ for the two cases are about 0.94548 and 1.25999, respectively; the corresponding eigenfunctions are reported in the second row of plots. The values of residuals (10) in infinity norm are 0.0018 and 0.64, respectively. The second residual is not so small. In fact, the first part of the numerical residual contains terms like $|\nabla u(x)|^{p(x)-1}$ (see (17)), with $\nabla u(x)$ close to zero where $p(x)$ is close to one. Those terms are approximated by $|\nabla u(x) + \mathcal{O}(h)|^{p-1}$, where h the mesh size, which can be quite far from their exact values. A possible confirmation of such an explanation is the fact that the maximum of the residual is taken at $\bar{x} = 0.04$, where $\nabla u(\bar{x}) \approx 0$ and $p(\bar{x}) = 1.1$. Similar values of the residuals were observed for the smaller values of p in the constant case.

3.3 Two-dimensional cases

We implemented and run the algorithm with FreeFem++ 3.23, using piecewise quadratic elements for $u(x,y)$ and piecewise constant elements for $p(x,y)$, in order to better manage discontinuous functions $p(x,y)$.

3.3.1 The rectangle

The initial solution $u^0(x,y)$ corresponding to $p(x,y) \equiv p = 2$ is the first eigenfunction of

$$-\nabla^2 u(x,y) = \eta_2 u(x,y), \quad x_0 < x < x_1, \ y_0 < y < y_1$$

normalized to have $\|u^0\|_2 = 1$, that is

$$u^0(x,y) = \sqrt{\frac{8}{(x_1-x_0)(y_1-y_0)}} \sin\left(\frac{x-x_0}{x_1-x_0}\pi\right) \sin\left(\frac{y-y_0}{y_1-y_0}\pi\right)$$

$$\eta_2 = \underline{\eta_2} = \left(\frac{\pi}{x_1-x_0}\right)^2 + \left(\frac{\pi}{y_1-y_0}\right)^2.$$

p	$\underline{\lambda}^p$	Ref. [13]	Ref. [9]
1.5	10.0722	10.0722	10.0720
2.0	19.7393	19.7392	19.7392
2.5	35.9490	35.9493	35.9487
4.0	176.618	176.693	176.598

**Table 2** Values of $\underline{\lambda}^p$ for some values of constant $p(x) \equiv p$.

For some constant values of $p(x) \equiv p$, Ref. [13, Table 4, p-version] reports the values of the eigenvalues $\underline{\lambda}^p$ with six significant digits for the unit square and Ref. [9, Table 2] reports the values for a wider range of p. In Table 2 we compare our results for $p = 1.5, 2, 2.5$ and 4.0 computed on a regular mesh with 26×26 vertices and 1250 triangles. We find that our

	precNewton(10)			precNLCG(10)		
	λ	residual	CPU s.	λ	residual	CPU s.
$p_1(x)$	4.0571	2.16e-4	38.46	4.0571	2.19e-4	84.42
$p_2(x)$	4.1727	2.51e-4	49.32	4.1727	2.52e-4	77.14

Table 3 Comparison for the cases $p_1(x,y) = 5 + 3\sin(3\pi x)$ and $p_2(x,y) = 4.5 + 3\sin(3\pi x)$.

results are closer to those obtained by the p-version of FEM algorithm used in Ref. [13] than to those obtained in Ref. [9].

In order to test the code performance, we compared our new minimization method (called `precNewton(10)` in Table 3) with the FreeFem++ function `NLCG`, which implements the nonlinear conjugate gradient minimization method (see Table 3). In a first example, taken from Ref. [6, Section 2.2], $p_1(x,y) = 5 + 3\sin(3\pi x)$. Here, differently than in Ref. [6], we implemented a preconditioner for the `NLCG` method based on modified Hessian (21) and set the maximum number of iterations to 10. Therefore, the method is denoted `precNLCG(10)` in Table 3. In a second example we checked the case $p_2(x,y) = 4.5 + 3\sin(3\pi x)$, in which $p_2(x,y)$ assumes values less than two. As shown in Table 3, our method outperforms the preconditioned `NLCG` in terms of CPU time (with comparable residuals).
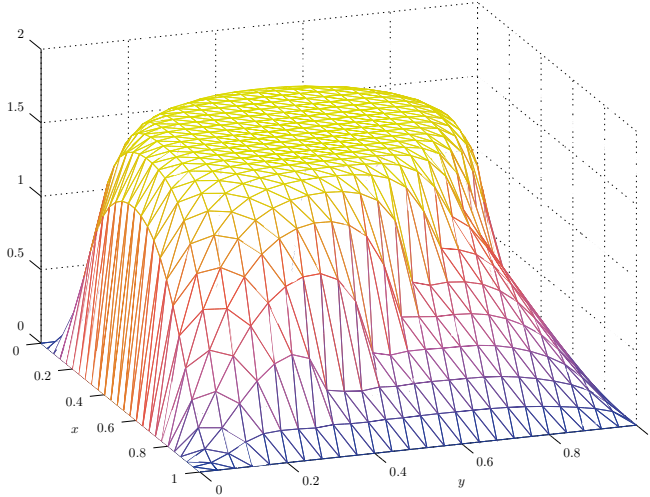
Fig. 3 Eigenfunction for $p_3(x,y)$. $\underline{\lambda} \approx 4.3491$, residual 0.16.

As a final test, we considered a discontinuous case with

$$p_3(x,y) = \begin{cases} 1.1 & \text{if } x^2 + y^2 \leq 1 \\ 10 & \text{otherwise} \end{cases}$$

The corresponding eigenfunction $u(x,y)$ is shown in Figure 3. Its shape resembles that of the one-dimensional case (see Figure 2, right).

3.3.2 The disk

We computed the eigenvalues for the disk for some constant values of $p(x) \equiv p$, namely $p = 1.5, 2, 2.5$ and 4. The initial solution $u^0(x, y)$ corresponding to $p(x, y) \equiv p = 2$ is the normalized first eigenfunction of

$$-\nabla^2 u(x,y) = \eta_2 u(x,y), \quad x^2 + y^2 < r^2$$

that is

$$u^0(x,y) = \frac{\tilde{u}^0(x,y)}{\|\tilde{u}^0\|_2}, \quad \tilde{u}^0(x,y) = J_0\left(j_{0,1}\frac{\sqrt{x^2+y^2}}{r}\right), \quad \eta_2 = \underline{\eta_2} = \left(\frac{j_{0,1}}{r}\right)^2$$

where J_0 is the Bessel function of the first kind of order zero and $j_{0,1} \approx 2.40482555769577$ is its first zero, computed by the commands

```
f = @(z) besselj(0,z);
fzero(f,[2,3],optimset("TolX",eps))
```

in GNU Octave 3.8. In Table 4 we compare our results for the unit disk ($r = 1$), on a mesh

p	$\underline{\lambda}^p$	Ref. [9]
1.5	4.0167	4.0053
2.0	5.7815	5.7616
2.5	7.7081	7.6815
4.0	14.6785	14.6369

Table 4 Values of $\underline{\lambda}^p$ for some values of constant $p(x) \equiv p$.

with 2032 vertices and 3912 triangles, with those provided in Ref. [9, Table 1] (there reported with five or six significant digits). We notice that for $p(x) \equiv 2$, the analytical solution is $j_{0,1}^2 \approx 5.7832$ and that our value is more accurate.

3.3.3 The annulus

The initial solution $u^0(x, y)$ corresponding to $p(x, y) \equiv p = 2$ for the annulus is the normalized first eigenfunction of

$$-\nabla^2 u(x,y) = \eta_2 u(x,y), \quad a^2 < x^2 + y^2 < b^2$$

that is

$$u^0(x,y) = \frac{\tilde{u}^0(x,y)}{\|\tilde{u}^0\|_2}, \quad \eta_2 = \underline{\eta_2} = \left(\frac{k_{0,1}}{a}\right)^2$$

where

$$\tilde{u}^0(x,y) = J_0(k_{0,1})Y_0\left(k_{0,1}\frac{\sqrt{x^2+y^2}}{a}\right) - Y_0(k_{0,1})J_0\left(k_{0,1}\frac{\sqrt{x^2+y^2}}{a}\right)$$

If we choose $a = 0.5$ and $b = 1$, then $k_{0,1} \approx 3.12303091959569$ is the first zero of

$$J_0(z)Y_0\left(z\frac{b}{a}\right) - Y_0(z)J_0\left(z\frac{b}{a}\right)$$

computed by the commands

```
a=0.5;,b=1;
f = @(z) besselj(0,z).*bessely(0,z*b/a)-bessely(0,z).*besselj(0,z*b/a);
fzero(f,[2,4],optimset("TolX",eps))
```

and Y_0 being the Bessel function of the second kind of order zero. The eigenvalues in Table 5

p	$\underline{\lambda}^p$	exact
1.5	14.8932	
2.0	38.9932	39.0133
2.5	95.0417	
4.0	1154.08	

Table 5 Values of $\underline{\lambda}^p$ for some values of constant $p(x) \equiv p$.

were obtained on a mesh with 1502 vertices and 2780 triangles. The exact value of $\underline{\eta}_2$ for the analytical known case $p(x) \equiv 2$ is $4k_{0,1}^2$.

4 Conclusions

We described an effective method for the computation of the first eigenpair of the $p(x)$-Laplacian problem. The numerical results, in one- and two-dimensional domains, agree well with those analytical or numerical available in literature for the constant case $p(x) \equiv p$. The main contribution of the present work is a fast and reliable method for the general case of variable exponent $p(x) \geq p^- > 1$, applied for the first time to some test problems in the critical range $p(x) < 2$ somewhere in the domain.

References

1. Acerbi E, Mingione G (2001) Regularity Results for a Class of Functionals with Non-Standard Growth. Arch Rational Mech Anal 156(2):121–140
2. Acerbi E, Mingione G (2005) Gradient estimates for the $p(x)$-Laplacean system. J reine angew Math 584:117–148
3. Akagi G, Matsuura K (2013) Nonlinear diffusion equations driven by the $p(\cdot)$-Laplacian. Nonlinear Differ Equ Appl 20:37–64
4. Astarita G, Marrucci G (1974) Principles of non-Newtonian fluid mechanics. McGraw-Hill
5. Atkinson C, Champion CR (1984) Some boundary value problems for the equation $\nabla \cdot (|\nabla \varphi|^N)$. Q J Mech Appl Math 37:401–419
6. Bellomi M, Caliari M, Squassina M (2013) Computing the first eigenpar for problems with variable exponents. J Fix Point Theory Appl 13(2):561–570
7. Biezuner RJ, Ercole G, Martins EM (2009) Computing the first eigenvalue of the p-Laplacian via the inverse power method. J Func Anal 257:243–270
8. Biezuner RJ, Ercole G, Martins EM (2011) Computing the $\sin_p$ function via the inverse power method. Comput Methods Appl Math 11(2):129–140

9. Biezuner RJ, Brown J, Ercole G, Martins EM (2012) Computing the First Eigenpair of the p-Laplacian via Inverse Iteration of Sublinear Supersolutions. J Sci Comput 52(1):180–201

10. Bird R, Armstrong R, Hassager O (1987) Dynamics of polymeric liquids, vol 1: Fluid mechanics, 2nd edn. John Wiley

11. Bognár G (2008) Numerical and analytic investigation of some nonlinear problems in fluid mechanics. In: Computers and Simulation in Modern Science, Vol. II., World Scientific and Engineering Academy and Society (WSEAS), pp 172–180

12. Bognár G, Rontó M (2005) Numerical-analytic investigation of the radially symmetric solutions for some nonlinear PDEs. Comput Math Appl 50:983–991

13. Bognár G, Szabó T (2003) Solving nonlinear eigenvalue problems by using p-version of FEM. Comput Math Appl 46(1):57–68

14. Breit D, Diening L, Schwarzacher S (2014) Finite element methods for the $p(x)$-Laplacian, arXiv:1311.5121v2 [math.NA]

15. Diaz JI, de Thelin F (1994) On a nonlinear parabolic problem arising in some models related to turbulent flows. SIAM J Math Anal 5(4):1085–1111

16. Diaz JI, Hernandez J (1997) On the multiplicity of equilibrium solutions to a nonlinear diffusion equation on a manifold arising in climatology. J Math Anal Appl 216:593–613

17. Diening L, Harjulehto P, Hästö P, Ruzicka M (2011) Lebesgue and Sobolev Spaces with Variable Exponents, Lect. Notes Math., vol 2017. Springer

18. Fan X, Zhang Q, Zhao D (2005) Eigenvalues of $p(x)$-Laplacian Dirichlet problem. J Math Anal Appl 302(2):306–317

19. Franzina G, Lindqvist P (2013) An eigenvalue problem with variable exponents. Nonlinear Anal 85:1–16

20. Glowinski R, Rappaz J (2003) Approximation of a nonlinear elliptic problem arising in a non-Newtonian fluid model in glaciology. Modél Math Anal Numér 37(1):175–186

21. Guan M, Zheng L (2006) The similarity solution to a generalized diffusion equation with convection. Adv Dyn Syst Appl 1(2):183–189

22. Harjulehto P, P Hästö P, Lê UV, Nuortio M (2010) Overview of differential equations with non-standard growth. Nonlinear Anal 72:4551–4574

23. Hein M, Bühler T (2011) An inverse power method for nonlinear eigenproblems with applications in 1-spectral clustering and sparse pca. In: Lafferty J, Williams CKI, Shawe-Taylor J, Zemel RS, Culotta A (eds) Advances in Neural Information Processing Systems 23: 24th Annual Conference on Neural Information Processing Systems 2010, Curran Associates, Inc., pp 847–855

24. Kawohl B (1990) On a family of torsional creep problems. J reine angew Math 410:1–22

25. Kawohl B, Fridman V (2003) Isoperimetric estimates for the first eigenvalue of the p-Laplace operator and the Cheeger constant. Comment Math Univ Carolin 44:659–667

26. Kelley CT (1999) Iterative Methods for Optimization, Frontiers in Applied Mathematics, vol 18. SIAM, Philadelphia

27. Mastorakis NE, Fathabadi H (2009) On the Solution of p-Laplacian for non-Newtonian fluid flow. WSEAS Trans Math 8(6):238–245

28. Pélissier MC, Reynaud ML (1974) Etude d'un modéle mathématique d'écoulement de glacier. C R Acad Sci - Sér I - Math 279:531–534

29. Philip JR (1961) N-diffusion. Aust J Phys 14:1–13

30. Showalter RE, Walkington NJ (1991) Diffusion of fluid in a fissured medium with microstructure. SIAM J Math Anal 22:1702–1722